Chromophores in phenylenevinylene-based conjugated polymers: Role of conformational kinks and chemical defects

Emmanuelle Hennebicq, Caroline Deleener, Jean-Luc Brédas, Gregory D. Scholes, and David Beljonne

Citation: J. Chem. Phys. **125**, 054901 (2006); doi: 10.1063/1.2221310
View online: http://dx.doi.org/10.1063/1.2221310
View Table of Contents: http://jcp.aip.org/resource/1/JCPSA6/v125/i5
Published by the American Institute of Physics.

Chromophores in phenylenevinylene-based conjugated polymers: Role of conformational kinks and chemical defects

Emmanuelle Hennebicq[a] and Caroline Deleener
Laboratory for Chemistry of Novel Materials and Center for Research in Molecular Electronics and Photonics, University of Mons-Hainaut, Place du Parc 20, B-7000 Mons, Belgium

Jean-Luc Brédas
School of Chemistry and Biochemistry and Center for Organic Photonics and Electronics, Georgia Institute of Technology, Atlanta, Georgia 30332-0400 and Laboratory for Chemistry of Novel Materials and Center for Research in Molecular Electronics and Photonics, University of Mons-Hainaut, Place du Parc 20, B-7000, Mons, Belgium

Gregory D. Scholes
Lash Miller Chemical Laboratories, University of Toronto, Saint-George Street 80, Toronto, Ontario, M5S 3H6 Canada

David Beljonne[b]
Laboratory for Chemistry of Novel Materials and Center for Research in Molecular Electronics and Photonics, University of Mons-Hainaut, Place du Parc 20, B-7000 Mons, Belgium and School of Chemistry and Biochemistry and Center for Organic Photonics and Electronics, Georgia Institute of Technology, Atlanta, Georgia 30332-0400

(Received 10 April 2006; accepted 15 June 2006; published online 1 August 2006)

The influence of chemical defects and conformational kinks on the nature of the lowest electronic excitations in phenylenevinylene-based polymers is assessed at the semiempirical quantum-chemical level. The amount of excited-state localization and the amplitude of through-space (Coulomb-like) versus through-bond (charge-transfer-like) interactions have been quantified by comparing the results provided by excitonic and supermolecular models. While excitation delocalization among conjugated segments delineated by the defects occurs in the acceptor configuration, self-confinement on individual chromophores follows from geometric relaxation in the excited-state donor configuration. The extent of excited-state localization is found to be sensitive to both the nature of the defect and the length of the conjugated chains. Implications for resonant energy transfer along conjugated polymer chains are discussed. © *2006 American Institute of Physics*. [DOI: 10.1063/1.2221310]

I. INTRODUCTION

Understanding the microscopic parameters that govern the dynamics of energy transfer processes in conjugated polymers such as poly(*p*-phenylenevinylene) (PPV) and its derivatives is of prime importance with regard to their use as active materials, e.g., in photovoltaic devices[1] or (bio)chemical sensing applications.[2] The charge generation efficiency in solar cells and the detection sensitivity in sensors rely on the ability of the photoinduced electronic excitations to diffuse through the polymer organic layer toward either dissociation zones (in the former case) or recognition sites (in the latter case). This requires funneling of the electronic excitations over large distances to well-defined target spots, which is *a priori* difficult to reconcile with the disordered structure of most conjugated polymers and the resulting random diffusion processes. Interestingly, phenylenevinylene-based polymers have been shown to yield a few orders of magnitude enhancement in sensing response with respect to molecules of related chemical structures.[2] This has been assigned to the collective nature of the electronic excitations in conjugated polymers (where a local perturbation, e.g., induced by the presence of an analyte molecule can lead to major modifications in the luminescence properties of the whole polymer chains)[3] and/or to the existence of efficient tunneling pathways driving the excitations to a small number of low-energy sites (such channels might for instance arise from conjugated segments brought in close intermolecular contacts via coiling of the polymer chains).[4] While the first scenario calls for strong couplings among the repeat units along fully conjugated polymer chains, the latter invokes the formation of spatially localized excited species that subsequently drift along or (more likely) between chains.

Although the nature of electronic excitations in conjugated polymers remains a matter of debate, the general view is that primary excitations can be pictured as bound electron-hole pairs dressed by lattice distortions.[5] In addition to the strong electron-phonon coupling typical of π-conjugated materials (i.e., strong coupling of electronic excitations to vibrations),[6] excited-state localization can also be induced by the presence of either conformational kinks[6,7] (e.g., large torsion angles along the backbone) or chemical defects.[8] These defects/kinks can lead to conjugation breaks that confine the

[a]Electronic mail: emmanuelle@averell.umh.ac.be
[b]Electronic mail: david@averell.umh.ac.be

electronic excitations over small subunits acting as individual chromophores. Such a multichromophoric picture has been successfully used to rationalize the photophysical features of PPV-based systems, including distinct line shapes and linewidths in optical absorption and emission spectra,[9] dispersive-like energy transport,[10] and intermittent single-chain fluorescence.[11] This view is also supported by the fact that the energy migration dynamics in these polymers can be well accounted for by models based on incoherent motions and multistep hops of excitations among segments of different lengths and hence excitation energies.[12] It implies that the electronic couplings between conjugated segments are small in comparison to the spectral linewidths, so that energy transfer occurs after full geometric relaxation over the initially excited (*donor*) chromophore. It is worth stressing, however, that this does not prevent the *acceptor* states (i.e., vertical electronic excitations from the ground-state geometry) to be possibly delocalized over several close-lying conjugated segments.[13]

According to this picture, the extent of excited-state wave-function delocalization is expected to evolve with time along the following sequence: (i) the photoexcitation process initially creates an excited species whose spatial extent is fixed by the relative magnitudes of electronic couplings versus inhomogeneous (static) disorder; (ii) fast vibrational thermalization, mainly driven by intramolecular geometric relaxation, then leads to self-localization of the excitations over single conformational subunits, as the homogeneous (dynamic) linewidths are usually larger than the electronic interactions. In phenylenevinylene-based conjugated polymers, coiling of the chains due to chemical defects and/or conformational kinks likely allows for significant electronic couplings between closely spaced conjugated segments recoiled next to one another. However, there is currently no full understanding of the extent to which the photoinduced excited species delocalize through such interacting subunits.

Therefore, it is our goal in this work to assess the impact of chemical defects and conformational kinks on the electronic communication along single polymer chains in model *p*-phenylenevinylene oligomers (OPVs). More specifically, we explore the influence on the nature of the lowest electronic excitations, of the presence in the vinylene units of: (i) sp^3-hybridized carbon sites; and (ii) *cis* double bonds, see the chemical structures in Fig. 1. Such defects have been identified experimentally in PPV-based material and are believed to play a major role in the three-dimensional structural organization of the polymer chains in solution: Nouwen *et al.* have demonstrated the presence of *cis*-linkages in PPV films and investigated the conformational changes undergone by the polymer in the presence of such defects on basis of cross-polarization/magic angle spinning[13] C NMR. The NMR spectra indicate a break-up of the polymer chains into OPV segments delineated by the *cis*-linkages as a result of the rotation of adjacent phenyl rings out of the plane formed by the vinylenic link.[14] This has been further supported by calculation of potential energy surfaces at the *ab initio* Hartree-Fock level for *all-trans* and *cis-trans* phenylenevinylene trimers.[15] Barbara *et al.* successfully rationalized the fluorescence anisotropy distribution observed experimentally by

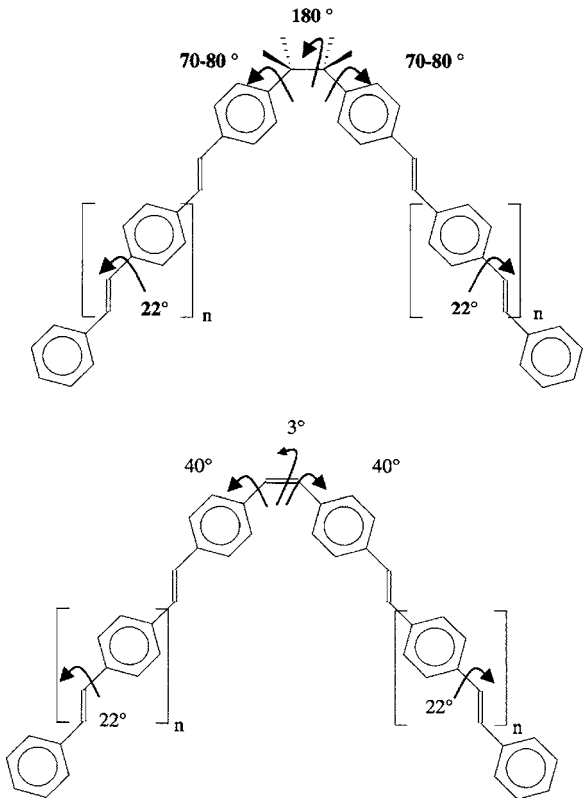

FIG. 1. Chemical structure of oligo(*p*-phenylenevinylene) segments including a *saturated* defect (top) and a *cis* linkage (bottom) along the backbone. The main features of the corresponding equilibrium ground-state geometries, as optimized at the AM1/CI level, are schematically illustrated as well. Arrows represent the torsion angles around the main single and double bonds along the polymer backbone.

performing Monte Carlo simulations on polymer chains including 5% of tetrahedral defects (i.e., single bonds that replace the C-C double bonds in phenylenevinylene backbone).[4,16] These tetrahedral kinks leading to the so-called "defect-coil" and "defect-cylinder" conformations might result from the presence of both *cis* double bonds and sp^3 defects, since the latter introduce a bond angle between the adjacent OPV segments similar to the tetrahedral one. The impact of such chemical defects on conformational disorder and polymer photophysics has been recently investigated by Hu *et al.* on the basis of single-molecule polarization spectroscopy measurements combined with Monte Carlo simulations of PPV chains with increasing amounts of tetrahedral defects. They evidenced a net decrease in conformational order and concomitantly a decrease in excitation diffusion length with increasing concentration of defects, which underlies the important role played by tetrahedral kinks in the energy transfer properties of phenylenevinylene-based conjugated polymers.[17]

It is worth pointing out that we have chosen to deal here with *intrachain*, i.e., through-bond, delocalization in short polymer chains. As pointed out earlier, through-space interactions could also lead to spreading of the electronic excitations over close-lying conjugated segments in long coil-like chains; these have, however, not been considered here.

II. THEORETICAL METHODOLOGY

A. Weak versus strong coupling: Excitonic model versus supermolecular approach

In order to get insight into the nature of the lowest-lying excited states in the acceptor and donor configurations of the model PPV chains including defects, correlated semiempirical quantum-chemical calculations have been performed on their electronic ground-state and excited-state geometries, respectively. Ground-state geometries were optimized using the semiempirical Austin Model 1 (AM1) technique.[18] This method has been successfully applied to similar systems by Rissler *et al.* and was shown to predict geometric structures in very good agreement with high-level *ab initio* (MP2/6-31G*) results[20] and x-ray diffraction data.[21]

The lowest-lying excited states were then computed on the basis of these geometries by means of the semiempirical Hartree-Fock INDO method[22] coupled with a single configuration interaction (SCI) technique.[23] The semiempirical Mataga-Nishimoto-Weiss potential has been adopted to describe the electron-electron interactions.[24] To ensure size-consistency, the CI active space was scaled with the number of carbon atoms by considering all the lowest unoccupied and highest occupied molecular orbitals (MOs) with dominant π character. In applying this procedure, 4 occupied and 4 unoccupied molecular orbitals were retained per phenylenevinylene unit. For instance, a CI active space including the 40 highest occupied and the 40 lowest unoccupied π-molecular orbitals has been used for the phenylenevinylene decamer (OPV_{10}). A detailed analysis of the lowest singlet excited states reveals that only the most frontier MOs (i.e., molecular orbitals with significant contribution on the ring para-carbons) contribute significantly to the lowest two singlet excited states, with the first one arising mostly from a simple highest occupied molecular orbital to lowest unoccupied molecular orbital electronic transition as reported previously.[25]

Geometric relaxation in the lowest singlet excited state has been investigated by combining the AM1 model to a CAS (complete active space) configuration-interaction formalism;[18] In the AM1 CI active space, singly excited electronic configurations with predominant contributions in the INDO/SCI expansion of the corresponding excited state were retained. Only a limited number of delocalized MOs were generally needed (1 occupied and 1 unoccupied delocalized molecular orbital per phenylenevinylene unit), i.e., the 10 highest occupied and 10 lowest unoccupied delocalized molecular orbitals in the case of the OPV_{10} molecule (these account for more than 98% of the total excited-state wave function).

To evaluate the regime of electronic coupling between excitations associated with the OPV segments located on both sides of the defect, we have compared the energy spectrum and the optical properties of the OPV molecules, as derived within the following two theoretical frameworks:

(i) The *excitonic model*[26–28] that only retains weak long-range Coulomb interactions between the chromophores, thereby assuming that the conjugated segments are separated by full conjugation breaks; this model thus only holds for weak coupling between OPV segments on both sides of the defect and

(ii) the *supermolecular approach*[28,29] where both short-range overlap and long-range Coulomb integrals are accounted for, making this approach valid for all coupling regimes.

In practice, this corresponds to applying in case (ii) a variational principle to the full chemical structure and the INDO Hamiltonian and in case (i) a perturbation formalism with the excited-state wave functions of the individual chromophores as zeroth-order wave functions and the interchromophoric Coulomb potential as the perturbation. In the excitonic model, the electronic couplings among excited states localized on two OPV conjugated segments have been obtained within a distributed monopole model[30] on the basis of INDO/SCI atomic transition densities.

Here, to assess the impact of structural and chemical defects on electronic communication along the conjugated chains, we focus on the simplest bichromophoric systems, i.e., OPV segments with increasing sizes including a single defect or kink, see Fig. 1. In the weak coupling limit, through-space or Coulomb-like interactions dominate and the two (excitonic and supermolecular) formalisms should yield similar results; in the strong coupling case, mixing with charge-transfer or through-bond configurations plays a significant role and the excitonic model is expected to break down.

B. Excitonic model

1. Basic concepts

The excitonic model is a physical concept originally developed by physicists to account for the delocalized character of excited states and to understand excitation-transfer process in crystals and supermolecules. This model has proved to be very useful in shedding light on the nature of electronic excitations in multichromophoric systems where electronic conjugation between the chromophores is interrupted. This is the case in van der Waals aggregates or supermolecules consisting of chromophores connected by aliphatic chains.

Excitonic models rely on the following two main approximations:

(i) The complete lack of electronic conjugation between the chromophores. Any exchange of electrons between the neighboring chromophores is thus ruled out, which implies a possible partitioning of the total system. The chromophores are interacting only through long-range Coulombic interactions. From this first assumption, it follows that charge-transfer states, which account for possible transfer of electronic density from one chromophore to another upon excitation (and can be pictured as split electron-hole pair states wherein oppositely charged particles reside on different physical sites), are neglected.

(ii) The assumption that intersite interactions, i.e., interactions between electronic excitations localized on different chromophores, remain small compared to

the intramolecular interactions taking place within each single chromophore. The coupling between monoexcited configurations associated to the same site is thus assumed to overwhelm the electronic coupling between monoexcited configurations associated to different sites. This is a central approximation in the theoretical descriptions relying on perturbation theory.

Within the excitonic model, the eigenfunctions of the bichromophore are expanded as linear combinations of monoexcited configurations localized on the two OPV sites, while neglecting any contribution of charge-transfer states and simultaneous excitations of both chromophores. In addition to the ground electronic state of the whole system, the relevant expansion functions to be considered are thus monoexcitations (localized excitations where a single chromophore is electronically excited—either to its first or higher-lying excited state—while the other chromophore lies in its ground state):

$$\begin{aligned} |\Psi_0^{(0)}\rangle &= |\psi_1^0\psi_2^0\rangle, \\ |\Psi_{1,1}^{(0)}\rangle &= |\psi_1^1\psi_2^0\rangle, \\ |\Psi_{2,1}^{(0)}\rangle &= |\psi_1^0\psi_2^1\rangle, \\ |\Psi_{1,n}^{(0)}\rangle &= |\psi_1^n\psi_2^0\rangle, \end{aligned} \tag{1}$$

where $|\psi_1^0\rangle, |\psi_1^1\rangle$, and $|\psi_1^n\rangle$ are the purely electronic ground-state, first, and nth excited-state wave functions localized on chromophore 1, respectively; $|\Psi_0^{(0)}\rangle$ represents the zeroth-order [as indicated by the (0) superscript] ground-state wave function of the supermolecule; $|\Psi_{1,1}^{(0)}\rangle$ is the excited supermolecular wave function where chromophore 1 is excited to its first singlet excited state (while the other OPV site resides in its electronic ground state) and $|\Psi_{1,n}^0\rangle$ corresponds to the electronic configuration arising from excitation of chromophore 1 to its nth excited state. All these configurations form a complete basis set within which the wave functions for the bichromophore can be expanded.

The calculation of the eigenstates of the bichromophoric compounds proceeds in two steps:

(i) The many-body energies and wave functions of the isolated chromophores (thus, completely neglecting the intersite interactions) are first evaluated at the INDO/SCI level.
(ii) The bichromophoric electronic states are then obtained by diagonalizing the excitonic matrix built on the basis of the electronic configurations in Eq. (1) and retaining only long-range interactions in the Hamiltonian.

The detailed description of the electronic ground and excited states of the bichromophoric systems, namely the corresponding transition energies and dipole moments, can be easily derived on the basis of the eigenvalues and eigenvectors of the excitonic matrix. The size of the basis set used to build the excitonic matrix, i.e., the number (n) of local electronic excitations per chromophore, has been adjusted to ensure convergence of the resulting excitation energies. Strong mixing between nondegenerate localized configurations can be expected provided their electronic coupling is large compared to the corresponding energy offset. In addition, degenerate configurations are expected to strongly mix together. Since we are only interested in the lowest singlet excited states of the bichromophoric entities, the proper electronic configurations to include in the CI basis are the lowest singlet excited configurations of the two chromophores (typically, four configurations per conjugated segment were accounted for).

2. Excitonic matrix elements

The detailed expression for the matrix elements of the excitonic Hamiltonian as well as the approximations considered in our model are described in the Appendix A. Here, we neglect polarization effects, i.e., the shift in excitation energies as well as the changes in electronic couplings among excited states as a result of relaxation of the electronic clouds induced by environment effects. The rigorous computation of polarization effects indeed represents a formidable task that requires the computation of charge (transition charge) distributions in (among) the electronic states of the individual chromophores in a self-consistent manner. Electrostatic interactions (computed on the basis of the state or transition charge distributions in the isolated molecules) have been calculated in a few test cases and turned out to bring only minor corrections to both the on- and off-diagonal elements of the excitonic matrix. They have therefore also been neglected throughout the work.

Overall, we have retained the electronic couplings between electronic excitations localized on different chromophore sites as off-diagonal elements and the excitation energies computed for the isolated molecules as diagonal elements of the excitonic Hamiltonian matrix. The electronic coupling between, e.g., the mth and nth excited states localized, respectively, on the first and second chromophore sites are expressed in terms of the atomic transition densities over the two chromophores [see Eq. (A38)]:

$$\langle \psi_1^n \psi_2^0 | \mathbf{H} | \psi_1^0 \psi_2^m \rangle = \frac{1}{4\pi\varepsilon_0} \sum_a \sum_b \rho_{0-n}^1(a) \rho_{0-m}^2(b) V(a,b), \tag{2}$$

with

$$\begin{aligned} \rho_{0-n}^1(a) &= \sum_{p\in a} \sum_{i,j\in 1} (\sqrt{2} C_{i,j}^{1,n} c_p^{1,i} c_p^{1,j}), \quad \rho_{0-m}^2(b) \\ &= \sum_{q\in b} \sum_{i',j'\in 2} \left(\sqrt{2} C_{i',j'}^{2,m} c_q^{2,i'} c_q^{2,j'}\right), \end{aligned} \tag{3}$$

where a and b run over all atomic sites on the first and second OPV segments; $V(a,b)$ is the Coulomb potential in atomic representation, which is taken here as the Mataga-Nishimoto[24] potential. $\rho_{0-n}^1(a)$ and $\rho_{0-m}^2(b)$ denote the transition densities on atomic sites a and b associated to the S_0-S_n and the S_0-S_m electronic transitions in the first and second OPV segments, respectively. Transition charges provide a local map of the transition dipole moment induced by an electronic excitation and can be viewed as a local

measure of the amount of electronic reorganization undergone by the system upon excitation.

The diagonal matrix element for the ground-state and excited-state $S_{1,n}$ configurations [see Eqs. (A28) and (A31)] when neglecting polarization effects is simply

$$\langle \Psi_0^{(0)}|H|\Psi_0^{(0)}\rangle = \langle \psi_1^0\psi_2^0|\mathbf{H}|\psi_1^0\psi_2^0\rangle + \langle \psi_1^0\psi_2^0|\mathbf{V}|\psi_1^0\psi_2^0\rangle \sim E_{1,0}^{(0)} + E_{2,0}^{(0)}, \quad (4)$$

$$\langle \psi_1^n\psi_2^0|\mathbf{H}|\psi_1^n\psi_2^0\rangle = \langle \psi_1^n\psi_2^0|\mathbf{H}_1^{(0)} + \mathbf{H}_2^{(0)}|\psi_1^n\psi_2^0\rangle + \langle \psi_1^n\psi_2^0|\mathbf{V}|\psi_1^n\psi_2^0\rangle \sim E_{1,n}^{(0)} + E_{2,0}^{(0)}, \quad (5)$$

where $\mathbf{H}_1^{(0)}(\mathbf{H}_2^{(0)})$ represents the zeroth-order Hamiltonian for isolated chromophore 1 (2); $\mathbf{V}$ is the perturbation operator accounting for intermolecular interactions between the two chromophores, i.e., here the Coulomb potential; $E_{1,0}^{(0)}$ and $E_{2,0}^{(0)}$ in Eq. (4) correspond to the zeroth-order ground-state energy associated to the first and second OPV segment; $E_{1,n}^{(0)}$ in Eq. (5) is the zeroth-order excitation energy computed at INDO/SCI level for the nth excited state.

C. Charge-transfer character: Electron-hole wave-function analysis

To characterize the excited-state wave functions, it is useful to define a quantity related to the joint probability of finding the hole and the electron of the excitation on specific atomic sites of the molecule (referred to as electron-hole wave function in the following).[19,31,32]

The electron-hole wave function can be expressed on the basis of the atomic orbital's (AOs) representation of the relevant reduced single-electron transition density matrix ρ^{0-1} (i.e., the electronic normal mode introduced by Mukamel *et al.*).[31] The elements of the transition density matrix $\rho_{q_i p_j}^{0-1} = \langle \Psi_1 | c_{p_j}^+ c_{q_i} | \Psi_0 \rangle$, where $c_{p_j}^+(c_{q_i})$ are the creation (annihilation) operators of one electron in AO $p_j(q_i)$, represent the joint amplitude of finding an extra electron on AO p_j and an extra-hole on AO q_i; p_j and q_i being centered on atoms p and q, respectively.

The probability for finding the hole on atomic center q and the electron on atom p, $\wp(p,q)$, can therefore be obtained by summing the relevant squared off-diagonal elements $(\rho_{p_j-q_i}^{0-1})^2$ of the transition densities $\Sigma_{p_j\in p}\Sigma_{q_i\in q}(\rho_{p_j-q_i}^{0-1})^2$. Within the SCI approximation considered here, $\wp(p,q)$ is

$$\wp(p,q) = \sum_{p_j\in p}\sum_{q_i\in q}\left|\sum_{a,r} C_a^r c_{a,q_i} c_{r,p_j}\right|^2, \quad (6)$$

where C_a^r is the configuration interaction (CI) expansion coefficient for the monoexcited configuration built by promoting one electron from occupied molecular orbital a to molecular orbital r; c_{a,p_j} and c_{r,q_i} are the LCAO coefficients of AOs p_j and q_i centered on atomic sites p and q in the MOs a and r, respectively. No additional symmetrization of the electron-hole wave function has thus been applied here, as previously proposed by Mukamel *et al.*[31] and Rissler *et al.*[19] and in contrast to previous studies.[33]

In order to evaluate the delocalization length of the electronic excitations, it is useful to quantify the relative contributions from the phenylenevinylene (PV) units and the possible defect. One can then partition the whole molecule into different physical subunits, namely in this case the different OPV segments and the defect itself, and compute the probabilities for finding the electron-hole pair within each subunit. The diagonal contributions $\wp_{\mathrm{OPV}_1}$, $\wp_{\mathrm{OPV}_2}$, and $\wp_{\mathrm{Def}}$ (i.e., configurations localized over specific subunits) to the electron-hole wave function read:

$$\wp_{\mathrm{OPV}_1} = \sum_{i\in \mathrm{OPV}_1} \wp_i \quad \text{with } \wp_i = \sum_{p,q\in i} \wp(p,q), \quad (7)$$

$$\wp_{\mathrm{OPV}_2} = \sum_{i\in \mathrm{OPV}_2} \wp_i \quad \text{with } \wp_i = \sum_{p,q\in i} \wp(p,q), \quad (8)$$

$$\wp_{\mathrm{Def}_1} = \sum_{p,q\in \mathrm{Def}} \wp(p,q), \quad (9)$$

where $\mathrm{OPV}_1(\mathrm{OPV}_2)$ denotes the first (second) OPV segment, Def refers to the defect, i labels the phenylenevinylene units in the OPV segments, and $\wp_i$ denotes the contribution of the repeat unit i to the squared electron-hole wave function. The localized character of the excitation can be evaluated by summing all the diagonal contributions to the electron-hole wave function as

$$\wp_{\mathrm{Loc}} = \sum_{p,q\in \mathrm{OPV}_1} \wp(p,q) + \sum_{p,q\in \mathrm{OPV}_2} \wp(p,q) + \sum_{p,q\in \mathrm{Def}} \wp(p,q). \quad (10)$$

The charge-transfer character is obtained by summing all the off-diagonal terms which accounts for the possibility of having the two particles on different subunits:

$$\wp_{\mathrm{C-T}} = \sum_{p\in \mathrm{OPV}_1}\sum_{q\in \mathrm{OPV}_2} \wp(p,q) + \sum_{p\in \mathrm{OPV}_1}\sum_{q\in \mathrm{Def}} \wp(p,q) + \sum_{p\in \mathrm{OPV}_2}\sum_{q\in \mathrm{Def}} \wp(p,q). \quad (11)$$

The different terms in Eq. (11) are associated to charge-transfer configurations arising from transfer of electronic density between the two OPV segments (first term), and from each OPV segment to the defect itself and vice-versa (second and third terms).

III. RESULTS AND DISCUSSION

A. Defect-free PPV chains

Before considering chains interrupted by conjugation defects, it is useful to look at the excited-state characteristics of long defect-free phenylenevinylene oligomers. The electron-hole density distributions computed at the INDO/SCI level on the basis of the ground-state and excited-state geometries of a 30-unit long all-*trans* OPV segment are displayed in Fig. 2. In the ground-state equilibrium configuration, the excitation is found to extend over a large fraction of the polymer chain (80% of the total wave function lies within the central 18 units). We note that: (i) what we are referring to here is the diagonal dimension related to the excitation delocalization (and not the off-diagonal size, which is a measure of the (much smaller) average electron-hole separation);[33] (ii) the

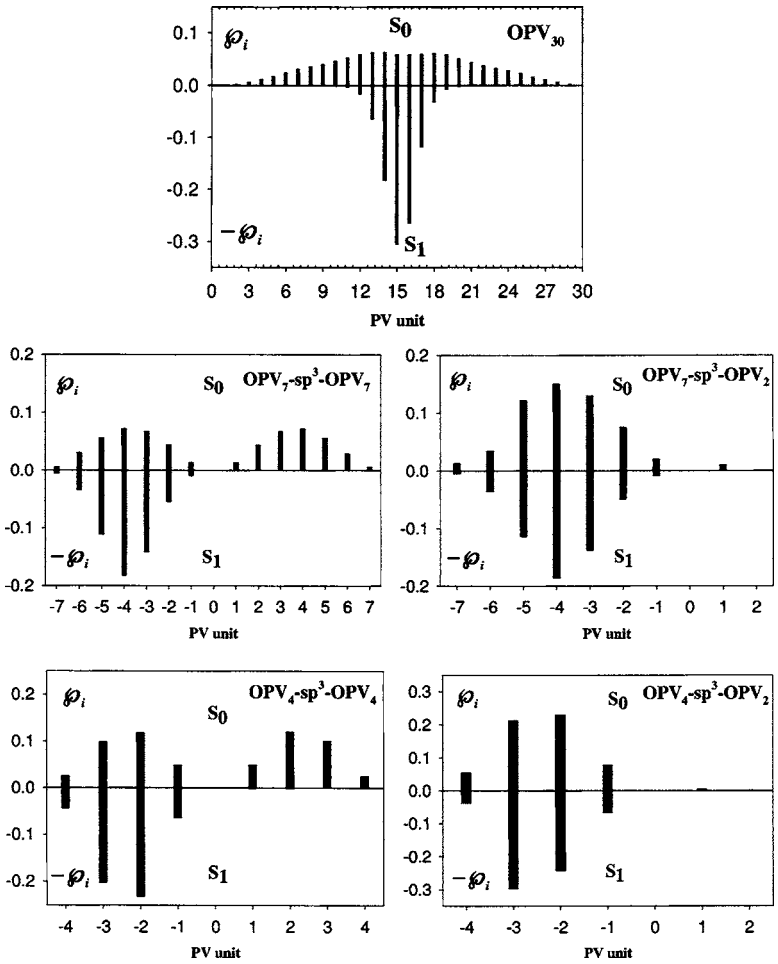

FIG. 2. Top: Electron-hole two-particle wave functions associated with the lowest singlet excited state of a defect-free 30-mer. The squared wave functions have been partitioned into contributions from each phenylenevinylene unit. The labels assigned to the latter range from 0 to 30 when moving from one edge of the oligomer to the other. Middle and bottom: Electron-hole two-particle wave functions associated with the lowest singlet excited state of molecules with sp^3 defects. The squared wave functions have been partitioned into contributions from each unit and the defect site itself [see Eqs. (7)–(9)]. On the abscissa, "0" refers to the defect site; negative values label the repeat units of the largest chromophore and positive values refer to the other chromophore. The influence of the degree of molecular asymmetry is investigated by comparing the results obtained for the totally symmetric and the most asymmetric systems in each series. In all cases, the impact of geometric relaxation phenomena is illustrated by comparison of the electronic wave functions computed in the ground-state (top y axis) and excited-state (bottom y axis) geometries.

extent of excitation delocalization is very sensitive to fluctuations in the torsion angles around the equilibrium values.[34] In the excited-state configuration, self-confinement of the lowest electronic excitation takes place over ~5 units around the central part of the conjugated chain whose geometric structure locally relaxes.

B. Chemical defects: sp^3-carbon atoms

We first address the case of PPV chains that include an sp^3 defect and lie in their ground-state (acceptor) configuration; chains ranging in size from 4 to 14 repeat units have been considered. As is the case for the butane molecule,[35] two minima have been identified on the AM1 ground-state potential energy curve of the compounds with a saturated defect: a staggered conformation (global minimum) and a *gauche* conformation (local minimum), see Fig. 1. INDO/SCI calculations have been performed for both types of structures; however, we only report here the results obtained on the most stable, staggered conformation.

Table I collects the lowest two singlet excitation energies computed within both the excitonic model and the supermolecular approach for one set of model chains with saturated defects and ranging in size from 9 to 14 phenylenevinylene repeat units. For all molecules investigated, the two models provide very similar vertical transition energies. This confirms that, as expected, saturated defects completely disrupt π-conjugation along the phenylenevinylene-based polymer chains.

A convenient way to analyze the electron-hole wave functions is to partition the full molecule into different conformational subunits (the two OPV branches and the defect) and to disentangle the contributions arising from local (LE) excitations (i.e., within the same subunit) to those corresponding to charge-transfer (CT) excitations (i.e., taking place between two distinct subunits), see methodology. From Table I and Fig. 2, it is clear that the lowest excited states in OPV molecules with sp^3 defects have a vanishingly small charge-transfer character, which is consistent with the fact that the excitonic and supermolecular models yield similar excitation energies.

In the fully symmetric cases (two OPV segments of identical lengths surrounding the defect), the lowest electronic excited states of the whole chain correspond to coherent superpositions of local excitations over the conjugated segments. The amount of excited-state wave-function delocalization over the whole molecule is determined by the trade-off between the rather significant through-space electronic couplings between excitations on the two sites (typically a few hundreds of wave numbers) and the energy offsets between the local excitations: As soon as some asymmetry is brought into the full system (e.g., when the two conjugated segments have slightly different lengths), the

TABLE I. Excitations energies for the lowest two singlet excited states in PV_7-sp^3-PV_n (top) and PV_7-*cis*-PV_n molecules (bottom), as computed on the basis of the excitonic model (EM) and the supermolecular approach (SA). The charge-transfer character in the lowest two excited states (percentage of the full two-particle density) is given between parentheses.

	EM		SA	
Chain	E_1 (cm^{-1})	E_2 (cm^{-1})	E_1 (cm^{-1})	E_2 (cm^{-1})
	sp^3 defect containing chains			
PV_7-*sat*-PV_7	26 540	26 730	26 500 (0)	26 720 (0.05)
PV_7-*sat*-PV_6	26 600	26 950	26 560 (0)	26 930 (0.09)
PV_7-*sat*-PV_5	26 620	27 370	26 580 (0)	27 310 (0.17)
PV_7-*sat*-PV_4	26 630	28 060	26 600 (0)	27 950 (0.32)
PV_7-*sat*-PV_3	26 630	28 830	26 600 (0)	28 690 (0.34)
PV_7-*sat*-PV_2	26 640	28 830	26 610 (0)	28 760 (0.25)
	cis-defect containing chains			
PV_7-*cis*-PV_7	26 520	26 740	26 085 (7.4)	26 730 (0)
PV_7-*cis*-PV_6	26 570	26 970	26 135 (7.2)	26 870 (0.9)
PV_7-*cis*-PV_5	26 600	27 360	26 190 (7.9)	27 050 (3.3)
PV_7-*cis*-PV_4	26 620	28 025	26 250 (7.9)	27 270 (7.6)
PV_7-*cis*-PV_3	26 620	28 730	26 310 (6.9)	27 560 (14.3)
PV_7-*cis*-PV_2	26 630	28 810	26 385 (5)	27 890 (16.8)

lowest excited state gets confined on the most conjugated chromophore, see Fig. 2. Thus, simultaneous excitation of several OPV segments separated by sp^3 chemical defects is expected to be strongly hindered by any source of inhomogeneity, such as conjugation-length distribution.

We now address the localization of the excited-state wave function taking place after thermal relaxation, i.e., in the equilibrium donor configuration. To quantify the geometric relaxations taking place in the excited state, the changes in C–C bond lengths when the chain goes from the ground-state geometry to the lowest excited-state geometry have been calculated first at the AM1/CAS-CI level. On the basis of the equilibrium geometries in the excited state, the INDO/SCI two-particle electron-hole wave functions have then been computed and partitioned into local and charge-transfer contributions as described earlier.

Geometric distortions induced by nuclear relaxations in both symmetric and asymmetric long chains are found to be completely localized over the most conjugated segment [see Fig. 3(a)]. At the same time, the excited-state wave function self-localizes on the distorted conjugated segment. This is illustrated by the topology of the computed electron-hole wave function, as pictured in Fig. 2. Note that, as is the case for the ground-state geometry, contributions from charge-transfer excitations across the saturated defect are negligible

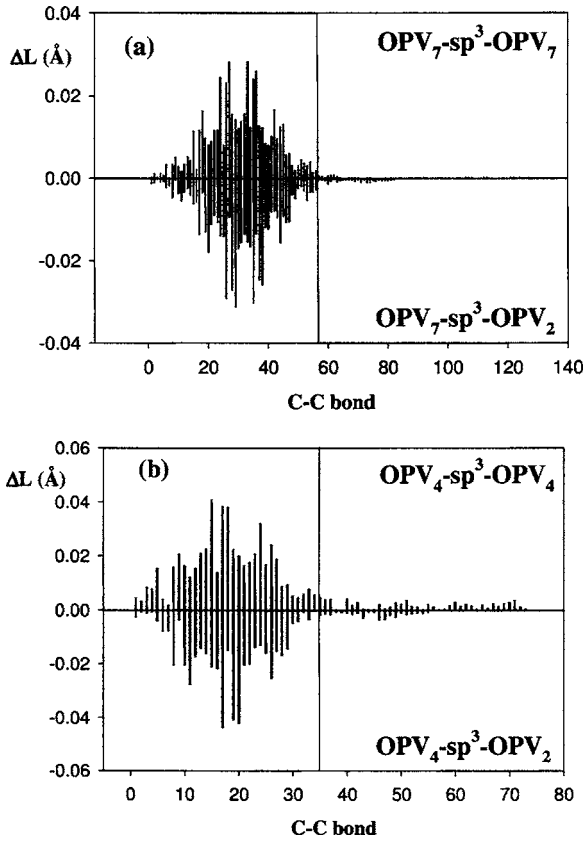

FIG. 3. Changes in C–C bond lengths upon geometric relaxation in the lowest excited state of molecules with sp^3 defects: $PV_{7\text{-}sp^3}$-PV_n (a) and $PV_{4\text{-}sp^3}$-PV_n (b).

in the excited-state geometry. In short chains (total chain length of 6–8 repeat units), a similar picture prevails; however, slight geometric deformations together with weak contributions to the excited-state wave functions are also predicted to occur on the less conjugated segment. We conjecture that such a "tunneling effect"[36] across the sp^3 defect arises because of the small size of the most extended conjugated segment, which is not large enough to accommodate the relaxed excited species (typical by extending over 5–6 OPV units).

Thus, except for very short conjugation lengths, the geometric relaxation in the excited state yields self-localized excited species in PPV chains that contain saturated defects. This is due to the large energy gain associated to the geometric reorganization (on the order of $\sim$2000 cm^{-1}) that largely exceeds the electronic coupling between the two chromophores.

C. Conformational kinks: *Cis* double bonds

In the OPV chains with *cis* defects, steric repulsions between the phenylene rings connected via the *cis* vinylene linkage leads to larger torsion angles around the single carbon-carbon bonds when compared to the all-*trans* structures: at the AM1 level, these amount to $\sim$40° and $\sim$22° in the fully optimized ground-state geometries, respectively. The AM1 value for the torsion angles around the double bond is $\sim$3°. These increased rotation angles around the single bonds in the vinylene groups should result in a re-

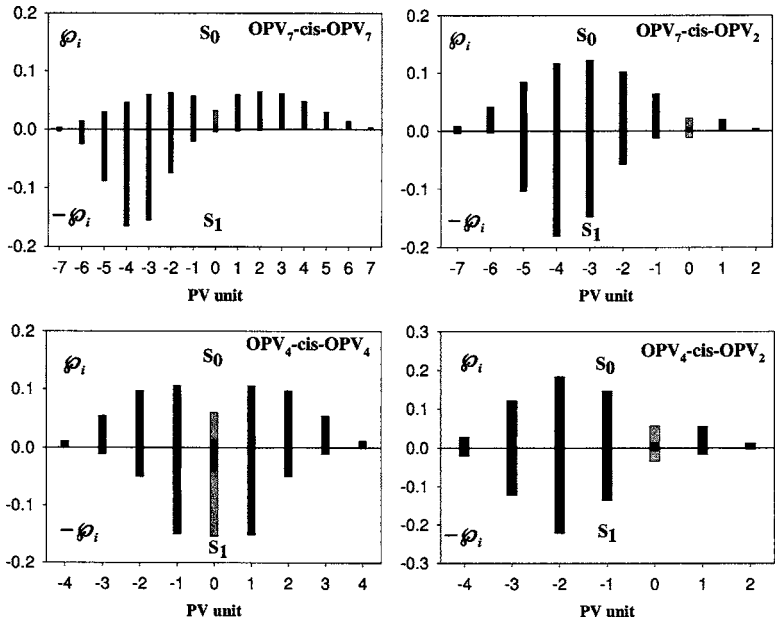

FIG. 4. Electron-hole two-particle wave functions associated with the lowest singlet excited state of molecules with a *cis* kink. Same as Fig. 2. Probability for finding both electron and hole within the same unit is shown as black vertical bars; grey bars represent the probability for finding one charged particle of the excitation on the defect site while the other resides on one OPV segment.

duced π-delocalization in PPV chains with *cis* defects. In order to check this statement, we applied the same procedure as that adopted for the saturated defects, to characterize the electronic excitations in chains containing a *cis* kink.

The electronic vertical transition energies computed for the lowest two singlet excited states at both excitonic and supermolecular levels are displayed in Table I. In contrast to what was obtained in the case of saturated defects, the two methods here yield very different results. For chains consisting of two OPV segments of the same or only slightly different length, a perfect match of the energetic positions predicted by the two models is obtained for the second excited state; on the other hand, excitation energies to the lowest excited state are found to strongly shift with respect to one another. The opposite trend is obtained for highly asymmetric systems: while similar excitation energies are given by the two methods for the first excited state, the second excited state obtained at the supermolecular level is strongly redshifted with respect to the corresponding state in the excitonic approach.

These results can be readily understood on the basis of a detailed analysis of the electron-hole wave functions (Fig. 4, top). In marked contrast with the sp^3-defect case, the INDO/SCI wave functions computed for the *cis* kink feature contributions on both sides of the *cis*-linkage together with smaller but sizable contributions on the kink itself; thus, charge-transfer contributions that account for the possible delocalization of the excitation across *cis* links here play a crucial role. Note that increasing the degree of molecular asymmetry induces a partial localization of the wave function on the most conjugated site (as a result of the energy offset between the two local excitations) with, however, slight residual contributions on the *cis* defect.

We are now in a position to rationalize the different excitation energies predicted by excitonic theory and the supermolecular approach. First, we note that the contributions from charge-transfer excitations to the supermolecular first [second] excited-state wave functions are found to decrease [increase] with increasing molecular asymmetry (see Table I). This can be understood in the following way (also recalling particle-in-the-box concepts). The lowest two excited states of the chains with a *cis* defect are in fact reminiscent of the corresponding states in the equivalent all-*trans* molecules (not shown): while the first excited-state wave function peaks around the central part of the system, the second excited-state wave function features two maxima separated by a node in the middle. Hence, in symmetric molecules, large [small] weights on the *cis*-vinylene linkage are obtained in the first [second] excited state, which thus shows a significant [negligible] charge-transfer character. Since, obviously, the larger the CT contributions, the larger the deviations between excitonic and supermolecular results, this explains why a much better agreement between the excitation energies predicted by the two models is attained for the second excited state. The same reasoning can be extended to asymmetric structures, where the opposite situation holds: smaller CT contributions to the two-particle wave functions are computed for the lowest-lying excited state, as the probability density is shifted away from the *cis*-vinylene site toward the geometric center of the molecule (see Fig. 4, top); hence, the closer match between excitonic and supermolecular results for the lowest transition energy in this case. In contrast, with increasing molecular asymmetry, the node in the second excited-state wave function drifts continuously off the *cis* defect toward the longest segment so that contributions on the *cis*-vinylene moiety are enlarged and the excitonic model yields less accurate transition energies.

Thus, although π-conjugation is reduced as a result of the increased torsion angles around the vinylene single bonds, chopping of the chains in their acceptor configuration (i.e., in the ground-state geometry) into chromophores separated by the *cis* kinks is in general not appropriate, as these act as single conjugated entities. In contrast to the saturated defect case, the energy disparity associated to the presence of all-*trans* segments of different sizes is not a strong enough perturbation to lift the coherence between the strongly

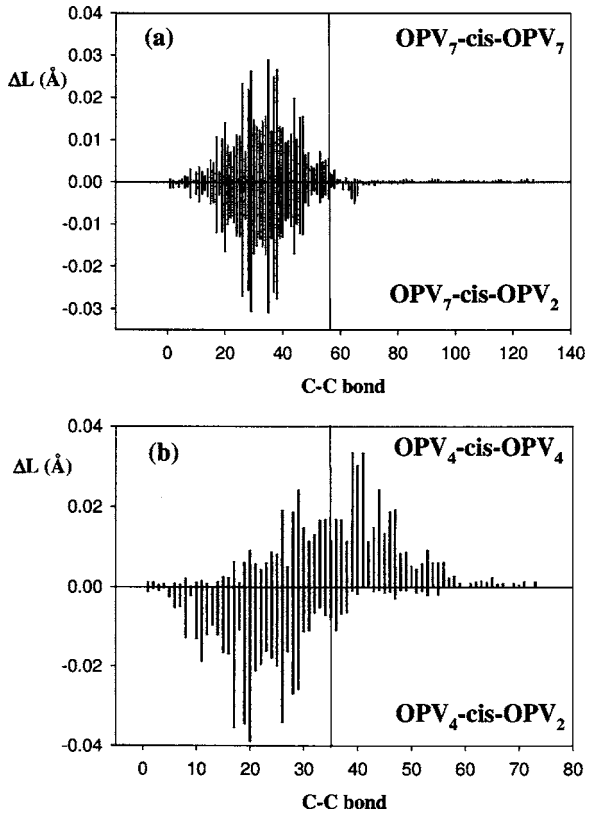

FIG. 5. Same as Fig. 3 for chains with a *cis* kink.

coupled conjugated units delineated by the *cis*-vinylene moieties. Hence, photoinduced excitation of PPV chains including vinylene groups in *cis* conformations is predicted to prepare extended excited species that spread out through the conformational kinks.

In a next step, we have investigated the geometric deformations taking place in the excited state and the resulting reshuffling in the excited-state wave functions for PPV chains with *cis* kinks. Here, different localization schemes are obtained for different lengths of the phenylenevinylene all-*trans* arms. In the longest systems investigated, i.e., OPV_7-*cis*-OPV_n series, we observe localization of the geometric distortions [Fig. 5(a)] and the resulting electron-hole wave functions (Fig. 4, top) over the most conjugated OPV segment (OPV_7) (with small but non-negligible contributions on the kink site). Thus, the energy gain induced by geometric relaxation process over the OPV_7 conjugated segment turns out to be large enough to overcome the delocalization energy conveyed by electronic coupling between the two sites. This is not the case for the shortest structures studied, i.e., the OPV_4-*cis*-OPV_n series, where strong electronic interactions between the two arms through the mediating *cis* vinylene bridge yield delocalized excitations in the excited-state equilibrium geometry [Fig. 4, bottom and Fig. 5(b)]. In these molecules, the largest deviations from the ground-state values are in fact obtained for the structural parameters pertaining to the *cis* vinylene units. In the intermediate-size chains, such as the OPV_5-*cis*-OPV_n series, the geometric distortion wave is found to be mainly localized on the OPV_5 segment while featuring a tail extending across the defect over the shortest *trans* segment [Fig. 5(b)]; a similar pattern is attained for the two-particle excited-state wave functions (Fig. 4, bottom).

With respect to the ground-state picture, geometric relaxation phenomena in the excited state tend to squeeze the wave functions to an extent that depends on the molecular length. While in long chains (for conjugated segments larger than ~5–6 repeat units) the donor states are localized on a single branch of the two-arm structures, the electronic excitations in short chains are centered around the *cis* conformational kinks (for conjugated segments shorter than ~4 repeat units).

IV. SYNOPSIS

The quantum-chemical studies presented here provide a detailed characterization of the amount of electronic excitation (de)localization in PPV-based conjugated chains containing either chemical defects or conformational kinks. More specifically, it allows us to identify the "donor" and "acceptor" chromophores involved in energy-migration processes in these polymers.

In the case of saturated defects (i.e., substitution with sp^3 carbon sites in the vinylene linkages), a weak-coupling model prevails, where geometric relaxation yields fully localized excited species on the single chromophores delineated by the defects. In the ground-state geometry, coherent excitation of multiple chromophores separated by the saturated vinylene moieties is possible in case of accidental degeneracy between the energy spectra of the chromophores. However, such a coherence is lost and the excitations get confined to single conjugated segments as soon as any source of energetic disorder, namely distribution in site energies, is introduced in the system.

In the case of *cis* kinks, partitioning of the whole system into chromophores is no longer possible, at least not in the acceptor configuration. Due to large charge-transfer interactions between conjugated segments across the *cis* linkages, the photoinduced excited species spread over the conformational kinks, even for large differences in segment lengths. Upon geometric relaxation in the excited state (thus, in the donor configuration), the amount of localization is found to depend on the chromophore size and the corresponding energy offset between localized excitations: For extended systems ($\geqslant$5 repeat units), self-confinement of the excited species over chain fragments separated by the kinks occurs, while in small chains geometric deformations and excited-state wave functions delocalize over the entire system.

The results presented here bear a strong impact on energy diffusion in flexible phenylenevinylene-based conjugated polymer chains. Assuming an average conjugation length in excess of five repeat units, a proper model to describe the dynamics of energy migration in such polymers should account for possible excitation delocalization across chemical defects and conformational kinks in the acceptor configuration and self-confinement on individual chromophores following geometric relaxation in the excited state. We have developed a modified Pauli master equation formalism that includes these features;[37] application of this approach to study energy transport in single PPV polymer

chains is in progress. Finally, we note that the calculations reported here strictly provide a 0 K temperature picture of the exciton delocalization. It is well known that the extent of self-trapping of excitons is greatly influenced by coupling to a fluctuating bath of nuclear modes, which we do not account for explicitly in the present work. Nonetheless, a steady-state description of the intramolecular reorganization is presented through geometry optimization of excited-state configurations. That provides a useful reference point for future work on the dynamics of exciton self-trapping and the influence of defects.

ACKNOWLEDGMENTS

The authors gratefully acknowledge the Belgian National Fund for Scientific Research (FNRS-FRFC) for its financial support. E.H. and D.B. are FNRS Postdoctoral Research Fellow and Research Associate, respectively. C.D. acknowledges a grant from FRIA ("Fonds pour la Formation à la Recherche dans 1'Industrie et dans 1'Agriculture"). The work at Georgia Tech is partly supported by the Office of Naval Research and the National Science Foundation (through the STC program under Award No. DMR-0120967 and Grant No. CHE-0342321). G.D.S. thanks the Natural Sciences and Engineering Research Council, Canada and the Alfred P. Sloan Foundation.

APPENDIX: EXCITONIC MATRIX ELEMENTS

General expressions for the ground-state ($|\Psi_1^0\rangle$) and the nth ($|\Psi_1^n\rangle$) singlet excited-state configurations over the first OPV segment read:[38,39]

$$|\Psi_1^0\rangle = |\Phi_1^0\rangle, \tag{A1}$$

$$|\Psi_1^n\rangle = \sum_{i,j\in 1} C_{i,j}^{1,n}\left(\frac{1}{\sqrt{2}} j_\uparrow^+ i_\uparrow + \frac{1}{\sqrt{2}} j_\downarrow^+ i_\downarrow\right)|\Phi_1^0\rangle, \tag{A2}$$

with

$$C_{i\uparrow,j\uparrow}^{1,n} = \frac{C_{i,j}^{1,n}}{\sqrt{2}} = C_{i\downarrow,j\downarrow}^{1,n}. \tag{A3}$$

Similarly, for the second OPV segment,

$$|\Psi_2^0\rangle = |\Phi_2^0\rangle, \tag{A4}$$

$$|\Psi_2^m\rangle = \sum_{i,j\in 2} C_{i,j}^{2,m}\left(\frac{1}{\sqrt{2}} j_\uparrow^+ i_\uparrow + \frac{1}{\sqrt{2}} j_\downarrow^+ i_\downarrow\right)|\Phi_2^0\rangle, \tag{A5}$$

$$C_{i\uparrow,j\uparrow}^{2,m} = \frac{C_{i,j}^{2,m}}{\sqrt{2}} = C_{i\downarrow,j\downarrow}^{2,m}, \tag{A6}$$

where $j_\downarrow^+(j_\uparrow^+)$ is the creation operator which creates an electron with spin up (spin down) in empty MO j while $i_\uparrow(i_\downarrow)$ represents the annihilation operator, which removes one electron with spin up (spin down) in MO i; $C_{i,j}^{1,n}$ ($C_{i,j}^{2,m}$) is the CI coefficient weighting the contribution from the monoexcited configuration resulting from a transition between occupied MO i and unoccupied MO j to the nth (mth) singlet excited state of the first (second) chromophore.

Next, MOs are expressed as linear combination of atomic orbitals according to[38,39]

$$\phi_{1,i} = \sum_p c_p^{1,i}\chi_{1,p}, \tag{A7}$$

$$\phi_{2,j} = \sum_q c_q^{2,j}\chi_{2,q}, \tag{A8}$$

wherein $\phi_{1,i}$ ($\phi_{2,j}$) is the ith (jth) MO in the first (second) OPV chromophore; $\chi_{1,p}(\chi_{2,q})$ is the AO $p(q)$ over the first (second) OPV chromophore; $c_p^{1,i}(c_q^{2,j})$ is the LCAO coefficient on atomic site $p(q)$ in MOs labeled i and j localized over the first (second) OPV site. In the following, general expressions for the matrix elements of the excitonic matrix are provided.

1. Diagonal matrix elements in the ground-state configuration

The diagonal matrix element for the ground-state configuration is

$$\begin{aligned}
&\langle\psi_1^0\psi_2^0|\mathbf{H}|\psi_1^0\psi_2^0\rangle \\
&\quad = \langle\psi_1^0\psi_2^0|\mathbf{H}_1^{(0)} + \mathbf{H}_2^{(0)}|\psi_1^0\psi_2^0\rangle + \langle\psi_1^0\psi_2^0|\mathbf{V}|\psi_1^0\psi_2^0\rangle \\
&\quad = E_{1,0}^{(0)} + E_{2,0}^{(0)} + \langle\psi_1^0\psi_2^0|\mathbf{V}|\psi_1^0\psi_2^0\rangle \\
&\quad = E_{1,0}^{(0)} + E_{2,0}^{(0)} + \sum_{k\in 1}\sum_{l\in 2}\langle\psi_1^0\psi_2^0|\frac{1}{4\pi\varepsilon_0 r_{kl}}|\psi_1^0\psi_2^0\rangle \\
&\quad = E_{1,0}^{(0)} + E_{2,0}^{(0)} + N_1N_2\langle\psi_1^0\psi_2^0|\frac{1}{4\pi\varepsilon_0 r_{kl}}|\psi_1^0\psi_2^0\rangle,
\end{aligned} \tag{A9}$$

wherein $|\psi_1^0\rangle$ ($|\psi_2^0\rangle$) is the zeroth-order ground-state wave function computed at the INDO/SCI level for the first (second) OPV segment; $\mathbf{H}_1^{(0)}(\mathbf{H}_2^{(0)})$ is the zeroth-order Hamiltonian describing the isolated first (second) OPV strand ($E_{1,0}^{(0)}$ and $E_{2,0}^{(0)}$ are the zeroth-order energies in the ground state of the two chromophores); $\mathbf{V}$ is the perturbation operator accounting for intermolecular interactions between the two chromophores, i.e., here the Coulomb potential. N_1 and N_2 represent the number of electrons for the first and second OPV segment; k and l label the electrons of chromophore 1 and 2, respectively.

Within the SCI formalism, the zeroth-order ground-state wave functions reduce to the Hartree-Fock determinants (in agreement with Brillouin's theorem according to which no coupling with singly excited configurations occurs) and one easily obtains for Eq. (A9):

$$N_1N_2\langle\psi_1^0\psi_2^0|\frac{1}{4\pi\varepsilon_0 r_{kl}}|\psi_1^0\psi_2^0\rangle = C\sum_{i\in 1}\sum_{j\in 2}[\phi_{1,i}\phi_{1,i}|\phi_{2,j}\phi_{2,j}]+[\bar{\phi}_{1,i}\bar{\phi}_{1,i}|\phi_{2,j}\phi_{2,j}] + [\phi_{1,i}\phi_{1,i}|\bar{\phi}_{2,j}\bar{\phi}_{2,j}]+[\bar{\phi}_{1,i}\bar{\phi}_{1,i}|\bar{\phi}_{2,j}\bar{\phi}_{2,j}] \quad \text{(A10)}$$

with

$$C=\frac{N_1N_2}{N_1!\,N_2!}(N_1-1)!\,(N_2-1)!=1, \quad \text{(A11)}$$

where i and j label occupied MOs in Hartree-Fock determinants associated to the first and second OPV segment, respectively; $\phi_{1,i}(\bar{\phi}_{1,i})$ represents the state of one electron with spin up (spin down) lying in molecular orbital $i.$; $[\phi_i\phi_j|\phi_k\phi_l]$ and other related terms correspond to Coulomb bielectronic integrals expressed in terms of spin-orbitals[38,39] and thus involving integration over both spatial and spin coordinates of the electrons:

$$[\phi_i\phi_j|\phi_k\phi_l] = \int d\mathbf{r}_1 d\mathbf{r}_2 d\omega_1 d\omega_2 \phi_i^*(\mathbf{r}_1)\alpha^*(\omega_1)\phi_j(\mathbf{r}_1)\alpha(\omega_1) \times\frac{1}{4\pi\varepsilon_0 r_{12}}\phi_k^*(\mathbf{r}_2)\alpha^*(\omega_2)\phi_l(\mathbf{r}_2)\alpha(\omega_2), \quad \text{(A12)}$$

$$[\phi_i\phi_j|\bar{\phi}_k\bar{\phi}_l] = \int d\mathbf{r}_1 d\mathbf{r}_2 d\omega_1 d\omega_2 \phi_i^*(\mathbf{r}_1)\alpha^*(\omega_1)\phi_j(\mathbf{r}_1)\alpha(\omega_1) \times\frac{1}{4\pi\varepsilon_0 r_{12}}\phi_k^*(\mathbf{r}_2)\beta^*(\omega_2)\phi_l(\mathbf{r}_2)\beta(\omega_2), \quad \text{(A13)}$$

where $\phi_i(\mathbf{r})$ represents the spatial molecular orbital i, $\alpha(\omega)$ and $\beta(\omega)$ the spin functions associated to the spin-up and spin-down state, respectively. The $N_1!$ and the $N_2!$ factors entering the prefactor C are the squared normalization factors associated to Slater determinants that contribute to the excited state of interest for the first and second OPV segment, respectively. The $(N_1-1)!((N_2-1)!)$ term represents the number of possible ways to permute the coordinates of the $N_1-1(N_2-1)$ remaining electrons of chromophore 1 (2) [whose position is not precised by the $\mathbf{r}_1(\mathbf{r}_2)$ coordinate entering the integrand].

This expression can be rewritten in a more compact way:

$$C\sum_{i\in 1}\sum_{j\in 2}[\phi_{1,i}\phi_{1,i}|\phi_{2,j}\phi_{2,j}]+[\bar{\phi}_{1,i}\bar{\phi}_{1,i}|\phi_{2,j}\phi_{2,j}] + [\phi_{1,i}\phi_{1,i}|\bar{\phi}_{2,j}\bar{\phi}_{2,j}]+[\bar{\phi}_{1,i}\bar{\phi}_{1,i}|\bar{\phi}_{2,j}\bar{\phi}_{2,j}] = 4\sum_{i\in 1}\sum_{j\in 2}(\phi_{1,i}\phi_{1,i}|\phi_{2,j}\phi_{2,j}), \quad \text{(A14)}$$

where $(\phi_i,\phi_j|\phi_k\phi_l)$ represents Coulomb bielectronic integrals expressed in terms of spatial molecular orbitals according to[38,39]

$$(\phi_i\phi_j|\phi_k\phi_l)=\int d\mathbf{r}_1 d\mathbf{r}_2\phi_i^*(\mathbf{r}_1)\phi_j(\mathbf{r}_1)\frac{1}{4\pi\varepsilon_0 r_{12}}\phi_k^*(\mathbf{r}_2)\phi_l(\mathbf{r}_2). \quad \text{(A15)}$$

By expanding the molecular orbitals entering Eq. (A14) as linear combination of atomic orbitals according to Eqs. (A7) and (A8), one finally gets

$$\begin{aligned}4\sum_{i\in 1}\sum_{j\in 2}(\phi_{1,i}\phi_{1,i}|\phi_{2,j}\phi_{2,j}) &= 4\sum_{i\in 1}\sum_{j\in 2}\sum_{p\in 1}\sum_{p'\in 1}\sum_{q\in 2}\sum_{q'\in 2}c_p^{1,i}c_{p'}^{1,i}c_q^{2,j}c_{q'}^{2,j}(\chi_{1,p}\chi_{1,p'}|\chi_{2,q}\chi_{2,q'})\\ &= 4\sum_{i\in 1}\sum_{j\in 2}\sum_{p\in 1}\sum_{p'\in 1}\sum_{q\in 2}\sum_{q'\in 2}c_p^{1,i}c_{p'}^{1,i}c_q^{2,j}c_{q'}^{2,j}\delta_{pp'}\delta_{qq'}(\chi_{1,p}\chi_{1,p}|\chi_{2,q}\chi_{2,q})\\ &= 4\sum_{i\in 1}\sum_{j\in 2}\sum_{p\in 1}\sum_{p'\in 1}\sum_{q\in 2}\sum_{q'\in 2}c_p^{1,i}c_{p'}^{1,i}c_q^{2,j}c_{q'}^{2,j}\delta_{pp'}\delta_{qq'}\frac{1}{4\pi\varepsilon_0}V(p,q)\\ &= \sum_{p\in 1}\sum_{q\in 2}\frac{\sum_{i\in 1}2(c_p^{1,i})^2\sum_{j\in 2}2(c_q^{2,j})^2}{4\pi\varepsilon_0}V(p,q), \end{aligned} \quad \text{(A16)}$$

wherein overlaps between different atomic orbitals $\chi_{1,p}\chi_{1,p},p\neq p'$ in the $(\chi_{1,p}\chi_{1,p'}|\chi_{2,q}\chi_{2,q'})$ terms have been neglected in compliance with the ZDO approximation assumed in INDO formalism,[40] and the two-electron two-center Coulomb integral $(\chi_{1,p}\chi_{1,p}|\chi_{2,q}\chi_{2,q})$ is evaluated from the Mataga-Nishimoto Coulomb potential $V(p,q)$.[24] The intermolecular interaction energy in the electronic ground state thus reduces to Coulomb interactions between atomic charges [hereafter denoted $\rho^1_{0-0}(a)$ and $p^2_{0-0}(b)$] in the ground-state of the two OPV segments:

$$\sum_{p\in 1}\sum_{q\in 2}\frac{\sum_{i\in 1}2(c_p^{1,i})^2\sum_{j\in 2}2(c_q^{2,j})^2}{4\pi\varepsilon_0}V(p,q)$$

$$=\sum_{a\in 1}\sum_{b\in 2}\left(\sum_{p\in a}\sum_{i\in 1}2(c_p^{1,i})^2\right)\left(\sum_{q\in b}\sum_{j\in 2}2(c_q^{2,j})^2\right)\frac{1}{4\pi\varepsilon_0}V(p,q)$$

$$=\sum_{a\in 1}\sum_{b\in 2}\frac{\rho^1_{0-0}(a)\rho^2_{0-0}(b)}{4\pi\varepsilon_0}V(a,b) \qquad \text{(A17)}$$

with

$$\rho^1_{0-0}(a)=\left(\sum_{p\in a}\sum_{i\in 1}2(c_p^{1,i})^2\right), \qquad \text{(A18)}$$

$$\rho^2_{0-0}(b)=\left(\sum_{q\in b}\sum_{j\in 2}2(c_q^{2,j})^2\right), \qquad \text{(A19)}$$

where a and b label atomic sites of the first and second OPV segments, respectively, and $V(a,b)\equiv V(p,q)$ is the Mataga-Nishimoto potential.

The whole matrix element is thus

$$\begin{aligned}\langle\Psi_0^{(0)}|H|\Psi_0^{(0)}\rangle &= \langle\psi_1^0\psi_2^0|\mathbf{H}|\psi_1^0\psi_2^0\rangle = \langle\psi_1^0\psi_2^0|\mathbf{H}_1^{(0)}+\mathbf{H}_2^{(0)}|\psi_1^0\psi_2^0\rangle \\ &\quad+\langle\psi_1^0\psi_2^0|\mathbf{V}|\psi_1^0\psi_2^0\rangle \\ &= E_{1,0}^{(0)}+E_{2,0}^{(0)}+\sum_{a\in 1}\sum_{b\in 2}\frac{\rho^1_{0-0}(a)\rho^2_{0-0}(b)}{4\pi\varepsilon_0}V(a,b). \qquad \text{(A20)}\end{aligned}$$

The first two terms in Eq. (A20) correspond to the zeroth-order energy of the system; the last term, which arises from Coulomb interactions between atomic charges in the electronic ground states of the chromophores, accounts for electrostatic interactions between the electronic clouds of the chromophores. Since these electrostatic terms were found to be negligible with respect to the zeroth-order energies (three orders of magnitude smaller on average), they have been neglected.

2. Diagonal matrix elements in the excited-state configuration

Using the expressions described in Eqs. (A1)–(A6) for the mth excited state of the bichromophore, one can write

$$\begin{aligned}\langle\psi_1^n\psi_2^0|\mathbf{H}|\psi_1^n\psi_2^0\rangle &= \langle\psi_1^n\psi_2^0|\mathbf{H}_1^{(0)}+\mathbf{H}_2^{(0)}|\psi_1^n\psi_2^0\rangle+\langle\psi_1^n\psi_2^0|\mathbf{V}|\psi_1^n\psi_2^0\rangle \\ &= E_{1,n}^{(0)}+E_{2,0}^{(0)}+\langle\psi_1^n\psi_2^0|\mathbf{V}|\psi_1^n\psi_2^0\rangle \\ &= E_{1,n}^{(0)}+E_{2,0}^{(0)}+\sum_{k\in 1}\sum_{l\in 2}\langle\psi_1^n\psi_2^0|\frac{1}{4\pi\varepsilon_0 r_{kl}}|\psi_1^n\psi_2^0\rangle. \qquad \text{(A21)}\end{aligned}$$

Applying the same procedure as in the previous section, we obtain

$$\begin{aligned}\langle\psi_1^n\psi_2^0|\mathbf{V}|\psi_1^n\psi_2^0\rangle = {} & C\sum_{i\in 1}\sum_{j\in 1}(C^{1,n}_{i\uparrow,j\uparrow})^2\sum_{l_{\text{doub.occ}}\in 1}\sum_{m\in 2}[\phi_{1,l}\phi_{1,l}|\phi_{2,m}\phi_{2,m}]+[\phi_{1,l}\phi_{1,l}|\bar\phi_{2,m}\bar\phi_{2,m}] \\ & + C\sum_{i\in 1}\sum_{j\in 1}(C^{1,n}_{i\uparrow,j\uparrow})^2\sum_{l_{\text{doub.occ}}\in 1}\sum_{m\in 2}[\bar\phi_{1,l}\bar\phi_{1,l}|\phi_{2,m}\phi_{2,m}]+[\bar\phi_{1,j}\bar\phi_{1,j}|\bar\phi_{2,m}\bar\phi_{2,m}] \\ & + C\sum_{i\in 1}\sum_{j\in 1}(C^{1,n}_{i\uparrow,j\uparrow})^2\sum_{m\in 2}[\phi_{1,i}\phi_{1,i}|\phi_{2,m}\phi_{2,m}]+[\phi_{1,i}\phi_{1,i}|\bar\phi_{2,m}\bar\phi_{2,m}] \\ & + C\sum_{i\in 1}\sum_{j\in 1}(C^{1,n}_{i\uparrow,j\uparrow})^2\sum_{m\in 2}[\phi_{1,j}\phi_{1,j}|\phi_{2,m}\phi_{2,m}]+[\phi_{1,j}\phi_{1,j}|\bar\phi_{2,m}\bar\phi_{2,m}] \\ & + C\sum_{i\in 1}\sum_{j\in 1}(C^{1,n}_{i\downarrow,j\downarrow})^2\sum_{l_{\text{doub.occ}}\in 1}\sum_{m\in 2}[\phi_{1,l}\phi_{1,l}|\phi_{2,m}\phi_{2,m}]+[\phi_{1,l}\phi_{1,l}|\bar\phi_{2,m}\bar\phi_{2,m}] \\ & + C\sum_{i\in 1}\sum_{j\in 1}(C^{1,n}_{i\downarrow,j\downarrow})^2\sum_{l_{\text{doub.occ}}\in 1}\sum_{m\in 2}[\bar\phi_{1,l}\bar\phi_{1,l}|\phi_{2,m}\phi_{2,m}]+[\bar\phi_{1,j}\bar\phi_{1,l}|\bar\phi_{2,m}\bar\phi_{2,m}] \\ & + C\sum_{i\in 1}\sum_{j\in 1}(C^{1,n}_{i\downarrow,j\downarrow})^2\sum_{m\in 2}[\bar\phi_{1,i}\bar\phi_{1,i}|\phi_{2,m}\phi_{2,m}]+[\bar\phi_{1,i}\bar\phi_{1,i}|\bar\phi_{2,m}\bar\phi_{2,m}] \\ & + C\sum_{i\in 1}\sum_{j\in 1}(C^{1,n}_{i\downarrow,j\downarrow})^2\sum_{m\in 2}[\bar\phi_{1,j}\bar\phi_{1,j}|\phi_{2,m}\phi_{2,m}]+[\bar\phi_{1,j}\bar\phi_{1,j}|\bar\phi_{2,m}\bar\phi_{2,m}] \\ & + C\sum_{i\in 1}\sum_{j\in 1}\sum_{j'\neq j,\in 1}C^{1,n}_{i\uparrow,j\uparrow}C^{1,n}_{i\uparrow,j'\uparrow}\sum_{m\in 2}[\phi_{1,j}\phi_{1,j'}|\phi_{2,m}\phi_{2,m}]+[\phi_{1,j}\phi_{1,j'}|\bar\phi_{2,m}\bar\phi_{2,m}] \\ & + C\sum_{i\in 1}\sum_{j\in 1}\sum_{j'\neq j,\in 1}C^{1,n}_{i\downarrow,j\downarrow}C^{1,n}_{i\downarrow,j'\downarrow}\sum_{m\in 2}[\bar\phi_{1,j}\bar\phi_{1,j'}|\phi_{2,m}\phi_{2,m}]+[\bar\phi_{1,j}\bar\phi_{1,j'}|\bar\phi_{2,m}\bar\phi_{2,m}]\end{aligned}$$

$$+ C\sum_{i\in 1}\sum_{i'\neq i,\in 1}\sum_{j\in 1} C^{1,n}_{i\uparrow,j\uparrow}C^{1,n}_{i'\uparrow,j\uparrow}\sum_{m\in 2}[\phi_{1,i}\phi_{1,i'}|\phi_{2,m}\phi_{2,m}] + [\phi_{1,i}\phi_{1,i'}|\bar{\phi}_{2,m}\bar{\phi}_{2,m}]$$

$$+ C\sum_{i\in 1}\sum_{i'\neq i,\in 1}\sum_{j\in 1} C^{1,n}_{i\downarrow,j\downarrow}C^{1,n}_{i'\downarrow,j\downarrow}\sum_{m\in 2}[\bar{\phi}_{1,i}\bar{\phi}_{1,i'}|\phi_{2,m}\phi_{2,m}] + [\bar{\phi}_{1,i}\bar{\phi}_{1,i'}|\bar{\phi}_{2,m}\bar{\phi}_{2,m}] \tag{A22}$$

where l runs over doubly occupied MOs of chromophore 1 in the monoexcited electronic configuration (as specified by the CI coefficient $C^{1,n}_{i,j}$) resulting from the promotion of one electron from molecular orbital i to molecular orbital j; m labels occupied MOs in ground-state configuration of chromophore 2. Equation (A22) can be further simplified:

$$\begin{aligned}\langle\psi^n_1\psi^0_2|\mathbf{V}|\psi^n_1\psi^0_2\rangle = &\sum_{i\in 1}\sum_{j\in 1}(C^{1,n}_{i,j})^2\sum_{l_{\text{doub.occ}}\in 1}\sum_{m\in 2}4(\phi_{1,l}\phi_{1,l}|\phi_{2,m}\phi_{2,m}) + \sum_{i\in 1}\sum_{j\in 1}(C^{1,n}_{i,j})^2\sum_{m\in 2}2(\phi_{1,i}\phi_{1,i}|\phi_{2,m}\phi_{2,m})\\ &+\sum_{i\in 1}\sum_{j\in 1}(C^{1,n}_{i,j})^2\sum_{m\in 2}2(\phi_{1,j}\phi_{1,j}|\phi_{2,m}\phi_{2,m}) + \sum_{i\in 1}\sum_{j\in 1}\sum_{j'\neq j,\in 1}(C^{1,n}_{i,j}C^{1,n}_{i,j'})\sum_{m\in 2}2(\phi_{1,j}\phi_{1,j'}|\phi_{2,m}\phi_{2,m})\\ &+\sum_{i\in 1}\sum_{i'\neq i,\in 1}\sum_{j\in 1}(C^{1,n}_{i,j}C^{1,n}_{i',j})\sum_{m\in 2}2(\phi_{1,i}\phi_{1,i'}|\phi_{2,m}\phi_{2,m}),\end{aligned} \tag{A23}$$

which can be rewritten in a more compact way:

$$\begin{aligned}&\sum_{i\in 1}\sum_{j\in 1}(C^{1,n}_{i,j})^2\sum_{k_{occ}\in 1}w^k_{i,j}\sum_{m\in 2}2(\phi_{1,k}\phi_{1,k}|\phi_{2,m}\phi_{2,m}) + \sum_{i\in 1}\sum_{j\in 1}\sum_{j'\neq j,\in 1}(C^{1,n}_{i,j}C^{1,n}_{i,j'})\sum_{m\in 2}2(\phi_{1,j}\phi_{1,j'}|\phi_{2,m}\phi_{2,m})\\ &\quad+\sum_{i\in 1}\sum_{i'\neq i,\in 1}\sum_{j\in 1}(C^{1,n}_{i,j}C^{1,n}_{i',j}),\sum_{m\in 2}2(\phi_{1,i}\phi_{1,i'}|\phi_{2,m}\phi_{2,m}),\end{aligned} \tag{A24}$$

where k runs over doubly and singly occupied MOs of chromophore 1 in the proper electronic configuration (as specified by the CI coefficient $C^{1,n}_{i,j}$); $w^k_{i,j}$ represents the occupation number of molecular orbital k in the monoexcited configuration resulting from the promotion of one electron from molecular orbital i to molecular orbital j.

MOs entering Eq. (A24) are then expanded as linear combination of atomic orbitals according to Eqs. (A7) and (A8). It follows:

$$\begin{aligned}\langle\psi^n_1\psi^0_2|\mathbf{V}|\psi^n_1\psi^0_2\rangle = &\sum_{i\in 1}\sum_{j\in 1}\sum_{p\in 1}\sum_{p'\in 1}(C^{1,n}_{i,j})^2\sum_{k_{occ}\in 1}w^k_{i,j}c^{1,k}_p c^{1,k}_{p'}\sum_{m\in 2}\sum_{q\in 2}\sum_{q'\in 2}2c^{2,m}_q c^{2,m}_{q'}(\chi_{1,p}\chi_{1,p'}|\chi_{2,q}\chi_{2,q'})\\ &+\sum_{i\in 1}\sum_{j\in 1}\sum_{j'\neq j,\in 1}\sum_{p\in 1}\sum_{p'\in 1}(C^{1,n}_{i,j}C^{1,n}_{i,j'})c^{1,j}_p c^{1,j'}_{p'}\sum_{m\in 2}\sum_{q\in 2}\sum_{q'\in 2}2c^{2,m}_q c^{2,m}_{q'}(\chi_{1,p}\chi_{1,p'}|\chi_{2,q}\chi_{2,q'})\\ &+\sum_{i\in 1}\sum_{i'\neq i,\in 1}\sum_{j\in 1}\sum_{p\in 1}\sum_{p'\in 1}(C^{1,n}_{i,j}C^{1,n}_{i',j})c^{1,i}_p c^{1,i'}_{p'}\sum_{m\in 2}\sum_{q\in 2}\sum_{q'\in 2}2c^{2,m}_q c^{2,m}_{q'}(\chi_{1,p}\chi_{1,p'}|\chi_{2,q}\chi_{2,q'}).\end{aligned} \tag{A25}$$

In the ZDO approximation, Eq. (A25) reduces to

$$\begin{aligned}&\sum_{i\in 1}\sum_{j\in 1}\sum_{p\in 1}\sum_{p'\in 1}(C^{1,n}_{i,j})^2\sum_{k_{\text{occ}}\in 1}w^k_{i,j}c^{1,k}_p c^{1,k}_{p'}\sum_{m\in 2}\sum_{q\in 2}\sum_{q'\in 2}2c^{2,m}_q c^{2,m}_{q'}\delta_{pp'}\delta_{qq'}\frac{1}{4\pi\varepsilon_0}V(p,q)\\ &\quad+\sum_{i\in 1}\sum_{j\in 1}\sum_{j'\neq j,\in 1}(C^{1,n}_{i,j}C^{1,n}_{i,j'})\sum_{p\in 1}\sum_{p'\in 1}c^{1,j}_p c^{1,j'}_{p'}\sum_{m\in 2}\sum_{q\in 2}\sum_{q'\in 2}2c^{2,m}_q c^{2,m}_{q'}\delta_{pp'}\delta_{qq'}\frac{1}{4\pi\varepsilon_0}V(p,q)\\ &\quad+\sum_{i\in 1}\sum_{i'\neq i,\in 1}\sum_{j\in 1}(C^{1,n}_{i,j}C^{1,n}_{i',j})\sum_{p\in 1}\sum_{p'\in 1}c^{1,i}_p c^{1,i'}_{p'}\sum_{m\in 2}\sum_{q\in 2}\sum_{q'\in 2}2c^{2,m}_q c^{2,m}_{q'}\delta_{pp'}\delta_{qq'}\frac{1}{4\pi\varepsilon_0}V(p,q)\\ &=\sum_{p\in 1}\sum_{q\in 2}\frac{\left(\sum_{i\in 1}\sum_{j\in 1}(C^{1,n}_{i,j})^2\sum_{k_{\text{occ}}}w^k_{i,j}(c^{1,k}_p)^2\right)\left(\sum_{m\in 2}2(c^{2,m}_q)^2\right)}{4\pi\varepsilon_0}V(p,q)\\ &\quad+\sum_{p\in 1}\sum_{q\in 2}\frac{\left(\sum_{i\in 1}\sum_{j\in 1}\sum_{j'\neq j,\in 1}(C^{1,n}_{i,j}C^{1,n}_{i,j'})c^{1,j}_p c^{1,j'}_p\right)\left(\sum_{m\in 2}2(c^{2,m}_q)^2\right)}{4\pi\varepsilon_0}V(p,q)\end{aligned}$$

$$+\sum_{p\in 1}\sum_{q\in 2}\frac{\left(\sum_{i\in 1}\sum_{i'\neq i,\in 1}\sum_{j\in 1}(C_{i,j}^{1,n}C_{i',j}^{1,n})c_p^{1,i}c_p^{1,i'}\right)\left(\sum_{m\in 2}2(c_q^{2,m})^2\right)}{4\pi\varepsilon_0}V(p,q). \tag{A26}$$

The orthonormality of spin orbitals involves $\Sigma_{p\in 1}c_p^{1,j}c_p^{1,j'}=\delta_{j,j'}$ and Eq (A26) becomes

$$\sum_{p\in 1}\sum_{q\in 2}\frac{\left(\sum_{i\in 1}\sum_{j\in 1}(C_{i,j}^{1,n})^2\sum_{k_{\mathrm{occ}}}w_{i,j}^{k}(c_p^{1,k})^2\right)\left(\sum_{m\in 2}2(c_q^{2,m})^2\right)}{4\pi\varepsilon_0}V(p,q). \tag{A27}$$

Equation (A27) can then be reorganized by regrouping terms involving AOs centered on the same atomic sites:

$$\sum_{p\in 1}\sum_{q\in 2}\frac{\left(\sum_{i\in 1}\sum_{j\in 1}(C_{i,j}^{1,n})^2\sum_{k_{\mathrm{occ}}}w_{i,j}^{k}(c_p^{1,k})^2\right)\left(\sum_{m\in 2}2(c_q^{2,m})^2\right)}{4\pi\varepsilon_0}V(p,q)$$

$$=\sum_{a\in 1}\sum_{b\in 2}\frac{\left(\sum_{p\in a}\sum_{i\in 1}\sum_{j\in 1}(C_{i,j}^{1,n})^2\sum_{k_{\mathrm{occ}}}w_{i,j}^{k}(c_p^{1,k})^2\right)\left(\sum_{m\in 2}\sum_{q\in b}2(c_q^{2,m})^2\right)}{4\pi\varepsilon_0}V(a,b)=\sum_{a\in 1}\sum_{b\in 2}\frac{\rho_{n-n}^{1}(a)\rho_{0-0}^{2}(b)}{4\pi\varepsilon_0}V(a,b) \tag{A28}$$

with

$$\rho_{n-n}^{1}(a)=\sum_{p\in a}\sum_{i\in 1}\sum_{j\in 1}(C_{i,j}^{1,n})^2\sum_{k_{\mathrm{occ}}}w_{i,j}^{k}(c_p^{1,k})^2 \tag{A29}$$

and

$$\rho_{0-0}^{2}(b)=\sum_{q\in b}\sum_{m\in 2}2(c_q^{2,m})^2, \tag{A30}$$

where $\rho_{n-n}^{1}(a)$ represent the atomic charges in the nth excited state of chromophore 1.

The diagonal matrix element for the excited configuration $S_{1,n}$ is finally

$$\langle\psi_1^n\psi_2^0|\mathbf{H}|\psi_1^n\psi_2^0\rangle$$
$$=E_{1,n}^{(0)}+E_{2,0}^{(0)}+\langle\psi_1^n\psi_2^0|\mathbf{V}|\psi_1^n\psi_2^0\rangle$$
$$=E_{1,n}^{(0)}+E_{2,0}^{(0)}+\sum_{a\in 1}\sum_{b\in 2}\frac{\rho_{n-n}^{1}(a)\rho_{0-0}^{2}(b)}{4\pi\varepsilon_0}V(a,b). \tag{A31}$$

The first two terms in Eq. (A31) correspond to the transition energies computed for the isolated chromophores; the last term accounts for the change in excitation energy resulting from electrostatic interactions between one OPV segment in its excited state and the other one in its ground state (electrostatic effect). Since these electrostatic terms were found to be negligible with respect to the zeroth-order energies in our case (three orders of magnitude smaller on average), they have been neglected.

3. Off-diagonal elements between ground-state and excited-state configurations

The relevant matrix element is

$$\langle\psi_1^n\psi_2^0|\mathbf{H}|\psi_1^0\psi_2^0\rangle=\langle\psi_1^n\psi_2^0|\mathbf{H}_1^{(0)}+\mathbf{H}_2^{(0)}|\psi_1^0\psi_2^0\rangle+\langle\psi_1^n\psi_2^0|\mathbf{V}|\psi_1^0\psi_2^0\rangle$$
$$=\langle\psi_1^n\psi_2^0|\mathbf{V}|\psi_1^0\psi_2^0\rangle$$
$$=\sum_{k\in 1}\sum_{l\in 2}\left\langle\psi_1^n\psi_2^0\left|\frac{1}{4\pi\varepsilon_0 r_{kl}}\right|\psi_1^0\psi_2^0\right\rangle. \tag{A32}$$

When expanding the zeroth-order electronic ground and excited states of the two OPV chromophores within the SCI formalism, one gets

$$\langle\psi_1^n\psi_2^0|\mathbf{V}|\psi_1^0\psi_2^0\rangle=C\sum_{i\in 1}\sum_{j\in 1}C_{i\uparrow,j\uparrow}^{1,n}\sum_{m\in 2}[\phi_{1,j}\phi_{1,i}|\phi_{2,m}\phi_{2,m}]+[\phi_{1,j}\phi_{1,i}|\bar{\phi}_{2,m}\bar{\phi}_{2,m}]+C\sum_{i\in 1}\sum_{j\in 1}C_{i\downarrow,j\downarrow}^{1,n}\sum_{m\in 2}[\bar{\phi}_{1,j}\bar{\phi}_{1,i}|\phi_{2,m}\phi_{2,m}]$$
$$+[\bar{\phi}_{1,j}\bar{\phi}_{1,i}|\bar{\phi}_{2,m}\bar{\phi}_{2,m}]=\sum_{i\in 1}\sum_{j\in 1}(C_{i\uparrow,j\uparrow}^{1,n}+C_{i\downarrow,j\downarrow}^{1,n})\sum_{m\in 2}2(\phi_{1,j}\phi_{1,i}|\phi_{2,m}\phi_{2,m})$$
$$=\sum_{i\in 1}\sum_{j\in 1}(\sqrt{2}C_{i,j}^{1,n})\sum_{m\in 2}2(\phi_{1,j}\phi_{1,i}|\phi_{2,m}\phi_{2,m}). \tag{A33}$$

By expanding the molecular orbitals entering Eq. (A33) as linear combination of atomic orbitals according to Eqs. (A7) and (A8), Eq. (A31) becomes

$$\sum_{i\in 1}\sum_{j\in 1}(\sqrt{2}C_{i,j}^{1,n})\sum_{m\in 2}2(\phi_{1,j}\phi_{1,i}|\phi_{2,m}\phi_{2,m})$$

$$=\sum_{i\in 1}\sum_{j\in 1}\sum_{p\in 1}\sum_{p'\in 1}(\sqrt{2}C_{i,j}^{1,n})c_p^{1,j}c_{p'}^{1,i}\sum_{m\in 2}\sum_{q\in 2}\sum_{q'\in 2}2c_q^{2,m}c_{q'}^{2,m}(\chi_{1,p}\chi_{1,p'}|\chi_{2,q}\chi_{2,q'})$$

$$=\sum_{i\in 1}\sum_{j\in 1}\sum_{p\in 1}\sum_{p'\in 1}(\sqrt{2}C_{i,j}^{1,n})c_p^{1,j}c_{p'}^{1,i}\sum_{m\in 2}\sum_{q\in 2}\sum_{q'\in 2}2c_q^{2,m}c_{q'}^{2,m}\delta_{pp'}\delta_{qq'}\frac{1}{4\pi\varepsilon_0}V(p,q)$$

$$=\sum_{p\in 1}\sum_{q\in 2}\frac{\left(\sum_{i\in 1}\sum_{j\in 1}(\sqrt{2}C_{i,j}^{1,n}c_p^{1,j}c_p^{1,i})\right)\left(\sum_{m\in 2}(2(c_q^{2,m})^2)\right)}{4\pi\varepsilon_0}V(p,q)$$

$$=\sum_{a\in 1}\sum_{b\in 2}\frac{\left(\sum_{p\in a}\sum_{i\in 1}\sum_{j\in 1}(\sqrt{2}C_{i,j}^{1,n}c_p^{1,j}c_p^{1,i})\right)\left(\sum_{q\in b}\sum_{m\in 2}(2(c_q^{2,m})^2)\right)}{4\pi\varepsilon_0}V(a,b)=\sum_{a\in 1}\sum_{b\in 2}\frac{\rho_{n-0}^1(a)\rho_{0-0}^2(b)}{4\pi\varepsilon_0}V(a,b) \tag{A34}$$

with

$$\rho_{n-0}^1(a)=\sum_{p\in a}\sum_{i\in 1}\sum_{j\in 1}(\sqrt{2}C_{i,j}^{1,n}c_p^{1,j}c_p^{1,i}) \tag{A35}$$

and

$$\rho_{0-0}^2(b)=\sum_{q\in b}\sum_{m\in 2}(2(c_q^{2,m})^2), \tag{A36}$$

where $\rho_{n-0}^1(a)$ denote the transition densities associated to the electronic transition from the ground state to the nth excited state of the first OPV segment and represent a local map of the corresponding transition dipole moment. These terms describe electrostatic interactions between transition charges induced by an electronic excitation on one chromophore and the ground-state charge densities on the other chromophore. These have also been neglected as they were found to be negligible (on average two orders of magnitude smaller, typically a few cm^{-1}) as compared to the terms accounting for mixing between localized excitations (typically several hundreds of cm^{-1}).

4. Off-diagonal elements between excited configurations

These elements can be regarded as a measure of the coupling between excited states of the system decoupled at order zero that may mix together upon application of the perturbation. Note that the coupling between excitations localized on the same chromophores is zero.

The relevant general expression for such matrix elements is

$$\langle\psi_1^n\psi_2^0|V|\psi_1^0\psi_2^m\rangle=\sum_{k\in 1,l\in 2}\left\langle\psi_1^n\psi_2^0\left|\frac{1}{r_{kl}}\right|\psi_1^0\psi_2^m\right\rangle$$

$$=C\sum_{i,j\in 1}\sum_{i',j'\in 2}(\sqrt{2}C_{i,j}^{1,n})(\sqrt{2}C_{i',j'}^{2,m})\times(\varphi_{1,j}\varphi_{1,i}|\varphi_{2,i'}\varphi_{2,j'})$$

$$=\sum_{i,j\in 1}\sum_{i',j'\in 2}(\sqrt{2}C_{i,j}^{1,n})(\sqrt{2}C_{i',j'}^{2,m})\times(\varphi_{1,j}\varphi_{1,i}|\varphi_{2,i'}\varphi_{2,j'}). \tag{A37}$$

Expanding the molecular orbitals entering Eq. (A37) as linear combination of atomic orbitals according to Eqs. (A7) and (A8) leads to

$$\sum_{i\in 1}\sum_{j\in 1}\sum_{p\in 1}\sum_{p'\in 1}(\sqrt{2}C_{i,j}^{1,n})c_p^{1,i}c_{p'}^{1,j}\sum_{i'\in 2}\sum_{j'\in 2}\sum_{q\in 2}\sum_{q'\in 2}(\sqrt{2}C_{i',j'}^{2,m})c_q^{2,i'}c_{q'}^{2,j'}[\chi_p\chi_{p'}|\chi_q\chi_{q'}]$$

$$=\sum_{i\in 1}\sum_{j\in 1}\sum_{p\in 1}\sum_{p'\in 1}(\sqrt{2}C_{i,j}^{1,n})c_p^{1,i}c_{p'}^{1,j}\sum_{i'\in 2}\sum_{j'\in 2}\sum_{q\in 2}\sum_{q'\in 2}(\sqrt{2}C_{i',j'}^{2,m})c_q^{2,i'}c_{q'}^{2,j'}\delta_{pp'}\delta_{qq'}\frac{1}{4\pi\varepsilon_0}V(p,q)$$

$$=\sum_{p\in 1}\sum_{q\in 2}\frac{\left(\sum_{i=1}\sum_{j\in 1}(\sqrt{2}C_{i,j}^{1,n})c_p^{1,i}c_p^{1,j}\right)\left(\sum_{i'\in 2}\sum_{j'\in 2}(\sqrt{2}C_{i',j'}^{2,m})c_q^{2,i'}c_q^{2,j'}\right)}{4\pi\varepsilon_0}V(p,q)$$

$$= \sum_a \sum_b \frac{\left(\sum_{p\in a}\sum_{i=1}\sum_{j\in 1}(\sqrt{2}C_{i,j}^{1,n})c_p^{1,i}c_p^{1,j}\right)\left(\sum_{q\in b}\sum_{i'\in 2}\sum_{j'\in 2}(\sqrt{2}C_{i',j'}^{2,m})c_q^{2,i'}c_q^{2,j'}\right)}{4\pi\varepsilon_0} V(a,b) = \sum_a \sum_b \frac{\rho_{0-n}^1(a)\rho_{0-m}^2(b)}{4\pi\varepsilon_0} V(a,b) \tag{A38}$$

with

$$\rho_{0-n}^1(a) = \sum_{p\in a}\sum_{i,j\in 1}(\sqrt{2}C_{i,j}^{1,n}c_p^{1,i}c_p^{1,j}), \tag{A39}$$

and

$$\rho_{0-m}^2(b) = \sum_{q=b}\sum_{i',j'\in 2}(\sqrt{2}C_{i',j'}^{2,m}c_q^{2,i'}c_q^{2,j'}). \tag{A40}$$

$\rho_{0-n}^1(a)$ and ρ_{0-m}^2 denote the transition densities on atomic sites a and b associated to the S_0-S_n and the S_0-S_m electronic transitions in the first and second OPV segments, respectively. Transition charges provide a local map of the transition dipole moment induced by an electronic excitation and can be viewed as a local measure of the amount of electronic reorganization undergone by the system upon excitation.

[1] A. Cravino and N. S. Sariciftci, J. Mater. Chem. **12**, 1931 (2002); A. J. Mozer, P. Denk, M. C. Scharber, H. Neugebauer, and N. S. Sariciftci, J. Phys. Chem. B **108**, 5235 (2004); H. Hoppe, M. Niggemann, C. Winder, J. Kraut, R. Hiesgen, A. Hinsch, D. Meissner, and N. S. Sariciftci, Adv. Funct. Mater. **14**, 1005 (2004).

[2] L. H. Chen, D. W. McBranch, H.-L. Wang, R. Hegelson, F. Wudl, and D. G. Whitten, Proc. Natl. Acad. Sci. U.S.A. **96**, 12287 (1999).

[3] T. D. McQuade, A. E. Pullen, and T. M. Swager, Chem. Rev. (Washington, D.C.) **100**, 2537 (2000); Q. Zhou and T. M. Swager, J. Am. Chem. Soc. **117**, 12593 (1995).

[4] D. Hu, K. Wong, B. Bagchi, P. J. Rossky, and P. F. Barbara, Nature (London) **405**, 1030 (2000).

[5] M. Pope and C. E. Swenberg, *Electronic Processes in Organic Crystals and Polymers* (Oxford University Press, New York, 1999).

[6] S. N. Yaliraki and R. J. Silbey, J. Chem. Phys. **104**, 1245 (1996).

[7] C. L. Gettinger, A. J. Heeger, J. M. Drake, and D. Pine J. Chem. Phys. **101**, 1673 (1994).

[8] G. D. Hale, S. J. Oldenburg, and N. J. Halas, Appl. Phys. Lett. **71**, 1483 (1997); T. Zyung and J. Kim, *ibid.* **67**, 3420 (1995).

[9] G. Padamanaban and S. Ramakrishnan J. Am. Chem. Soc. **122**, 2244 (2000).

[10] U. Rauscher, H. Bässler, D. D. C. Bradley, and M. Hennecke, Phys. Rev. B **42**, 9830 (1990); B. Mollay, U. Lemmer, R. Kersting, R. F. Mahrt, H. Kurz, H. F. Kauffmann, and H. Bässler, *ibid.* **50**, 10769 (1994); J. Sperling, F. Milota, A. Tortschanoff, and Ch. Warmuth, J. Chem. Phys. **117**, 10877 (2002).

[11] J. Yu, D. Hu, and P. F. Barbara, Science **289**, 1327 (2000).

[12] M. A. Summers, P. R. Kemper, J. E. Bushnell, M. R. Robinson, G. C. Bazan, M. T. Bowers, and S. T. Buratto, J. Am. Chem. Soc. **125**, 5199 (2003); M. Wind, U.-M. Wiesler, K. Saalwachter, K. Mullen, and H. W. Spiess, Adv. Mater. (Weinheim, Ger.) **13**, 752 (2001).

[13] G. R. Fleming and G. D. Scholes, Nature (London) **431**, 256 (2004).

[14] J. Nouwen, D. Vanderzande, H. Martens, J. Gelan, Z. Yang, and H. Geise, Synth. Met. **46**, 23 (1992); J. Nouwen, D. Vanderzande, H. Martens, and J. Gelan, *ibid.* **41–43**, 305 (1991).

[15] G. C. Claudio and E. R. Bittner, Chem. Phys. **276**, 81 (2002).

[16] P. F. Barbara, A. J. Gesquiere, S.-J. Park, and Y. J. Lee Acc. Chem. Res. **38**, 602 (2005); Z. Yu and P. F. Barbara, J. Phys. Chem. B **108**, 11321 (2004); K. F. Wong, M. S. Skaf, C.-Y. Yang, P. J. Rossky, B. Bagchi, D. Hu, J. Yu, and P. F. Barbara, *ibid.* **105**, 6103 (2001).

[17] D. H. Hu, J. Yu, G. Padmanaban, S. Ramakrishnan, and P. F. Barbara, Nano Lett. **2**, 1121 (2002).

[18] M. J. S. Dewar, E. G. Zoebisch, E. F. Healy, and J. J. P. Stewart, J. Am. Chem. Soc. **107**, 3702 (1995); D. R. Hartree, Proc. Cambridge Philos. Soc. **24**, 328 (1928). Within this formalism, excited states are obtained by performing a full-CI calculation over an active space including the molecular orbitals that form the most frontier π-delocalized electronic bands.

[19] J. Rissler, H. Bässler, F. Gebhard, and P. Schwerdtfeger, Phys. Rev. B **64**, 045122 (2001).

[20] C. Møller and M. S. Plesset, Phys. Rev. **46**, 618 (1934).

[21] C. J. Finder, M. G. Newton, and N. L. Allinger, Acta Crystallogr. **30**, 411 (1974); J. Cornil, D. Beljonne, D. A. Dos Santos, Z. Shuai, and J. L. Brédas, Synth. Met. **78**, 209 (1996).

[22] J. A. Pople, D. L. Beveridge, and P. A. Dobosch, J. Chem. Phys. **47**, 2026 (1967).

[23] V. Z. Fock, Phys. **61**, 126 (1930); J. Ridley and M. C. Zerner, Theor. Chim. Acta **32**, 111 (1973); M. C. Zerner, G. H. Loew, R. F. Kichner, and V. T. Mueller-Westerhoff, J. Am. Chem. Soc. **102**, 5279 (1980).

[24] N. Malaga and K. Nishimoto, Z. Phys. Chem. (Leipzig) **13**, 140 (1957); R. Pariser and R. Parr, J. Chem. Phys. **21**, 767 (1953).

[25] J. Cornil, D. Beljonne, R. H. Friend, and J. L. Brédas, Chem. Phys. Lett. **223**, 82 (1994).

[26] J. Frenkel, Phys. Rev. **37**, 1276 (1931); A. S. Davydov, *Theory of Molecular Excitons* (Plenum, New York, 1971).

[27] D. Markovitsi, A. Germain, P. Millié, P. Lécuyer, L. K. Gallos, P. Argyrakis, H. Bengs, and H. Ringsdorf, J. Phys. Chem. **99**, 1005 (1995).

[28] D. Beljonne, J. Cornil, R. Silbey, P. Millié, and J. L. Brédas, J. Chem. Phys. **112**, 4749 (2000).

[29] G. D. Scholes, I. R. Gould, R. J. Cogdell, and G. R. Fleming, J. Phys. Chem. B **103**, 2453 (1999).

[30] E. Hennebicq, G. Pourtois, G. D. Scholes *et al.*, J. Am. Chem. Soc. **127**, 4744 (2005).

[31] S. Mukamel, S. Tretiak, T. Wagersreiter, and V. Cherayak, Science **277**, 781 (1997); I. Franco and S. Tretiak, J. Am. Chem. Soc. **126**, 12130 (2004); S. Tretiak and S. Mukamel, Chem. Rev. (Washington, D.C.) **102**, 3171 (2002).

[32] L. Romaner, G. Heimel, H. Wiesenhofer, P. S. De Freitas, U. Scherf, J.-L. Brédas, E. Zojer, and E. J. W. List, Chem. Mater. **16**, 4667 (2004).

[33] E. Zojer, P. Buchacher, F. Wudl, J. Cornil, J. P. Calbert, J. L. Brédas, and G. Leising, J. Chem. Phys. **113**, 10002 (2000).

[34] C. Deleneer *et al.* (unpublished).

[35] J. B. Hendrickson, D. J. Cram, and G. S. Hammond, *in Organic Chemistry* (McGraw-Hill, New York, 1970), Chap. 6.

[36] A. H. A. Clayton, K. P. Ghiggino, G. J. Wilson, and M. N. Paddon-Row, J. Chem. Soc. A **97**, 7962 (1993).

[37] D. Beljonne, E. Hennebicq, C. Daniel *et al.*, J. Phys. Chem. B **109**, 10594 (2005).

[38] A. Szabo and N. S. Ostlund, *Modern Quantum Chemistry: Introduction to Advanced Electronic Structure Theory* (McGraw-Hill, New York, 1989).

[39] R. McWeeny, *Methods of Molecular Quantum Mechanics*, 2nd ed. (Academic, London, 2001).

[40] P. W. Atkins and R. S. Friedman, *Molecular Quantum Mechanics*, 3rd ed. (Oxford University Press, New York, 1997).